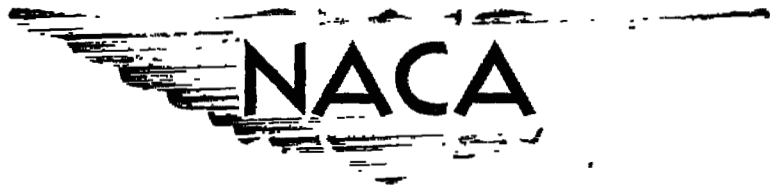


NACA RM L58B07

UNCLASSIFIED

C 2



NACA

RESEARCH MEMORANDUM

AERODYNAMIC CHARACTERISTICS OF A CANARD AND AN
OUTBOARD-TAIL AIRPLANE MODEL AT
A MACH NUMBER OF 2.01

By M. Leroy Spearman and Ross B. Robinson

Langley Aeronautical Laboratory
CLASSIFICATION CHANGED Langley Field, Va.

LIBRARY COPY

UNCLASSIFIED

MAR 21 1958

LANGLEY AERONAUTICAL LABORATORY
LIBRARY, NACA
LANGLEY FIELD, VIRGINIA

To _____

By authority of JNA #48 Date 5-29-61
com

CLASSIFIED DOCUMENT

This material contains information affecting the National Defense of the United States within the meaning of the espionage laws, Title 18, U.S.C., Secs. 793 and 794, the transmission or revelation of which in any manner to an unauthorized person is prohibited by law.

NATIONAL ADVISORY COMMITTEE FOR AERONAUTICS

WASHINGTON

March 24, 1958

UNCLASSIFIED

CONFIDENTIAL

UNCLASSIFIED

NATIONAL ADVISORY COMMITTEE FOR AERONAUTICS

RESEARCH MEMORANDUM

AERODYNAMIC CHARACTERISTICS OF A CANARD AND AN
OUTBOARD-TAIL AIRPLANE MODEL AT
A MACH NUMBER OF 2.01

By M. Leroy Spearman and Ross B. Robinson

SUMMARY

An investigation has been conducted in the Langley 4- by 4-foot supersonic pressure tunnel at a Mach number of 2.01 to determine the stability and control characteristics of a canard airplane configuration and an outboard-tail configuration. The canard model had a 67° swept wing with an aspect ratio of 2.17 and a trapezoidal canard control surface. The outboard-tail model had boom-mounted horizontal-tail controls located to the rear and outboard of the wing tips. This configuration was evolved from the same body wing used for the canard model but with the outer 30 percent of the wing span sheared back to form the horizontal-tail panels. The canard model had a single body-mounted vertical tail whereas the outboard-tail model had twin boom-mounted vertical tails with the same total exposed area as the canard model tail.

The results indicated relatively high values of maximum trimmed lift-drag ratio L/D for both configurations. The values of maximum trim lift-drag ratio L/D decreased as the stability level increased for both configurations, although the variation was less for the outboard-tail model than for the canard model. The values of trim L/D were higher in the low-lift range and the maximum L/D occurred at a lower lift coefficient for the canard configuration than for the outboard-tail configuration. At higher lift coefficients the values of trim L/D became higher for the outboard-tail configuration. These effects reflect the drag characteristics of the two configurations in that the outboard-tail configuration had a higher minimum drag but a lower drag due to lift than the canard configuration.

CONFIDENTIAL

UNCLASSIFIED


INTRODUCTION


The attainment of high values of lift-drag ratio for airplanes is essential from the range standpoint; however, sufficiently high values are sometimes difficult to obtain when trimming at supersonic speeds. The effects of trimming on lift-drag ratio are, of course, directly related to the level of longitudinal stability, the effects being less as the stability level decreases. For a given level of stability, however, the effect of trimming on the lift-drag ratio is dependent on the geometry of the configuration, particularly in relation to the type of pitch control system employed. Obviously, a desirable control system would be one that, when used for trimming, provided positive lift with a minimum of drag. Positive lift implies an upload from the control whereas a minimum of drag implies small controls, small deflections, or a forward inclination of the resultant force vector on the control.

In trimming a stable tailless configuration with wing trailing-edge flap controls, a download is required from the control. Thus, in order to trim at a given lift, a higher angle of attack with an attendant drag increase is required, and the result is a reduction in the lift-drag ratio.

Conventional tail-rearward airplanes, on the other hand, may be trimmed with either an upload or a download at the tail, depending upon whether the configuration is stable with the tail off. Such configurations at subsonic speeds are usually unstable with the tail off and thus require an upload from the control. However, because of the large downwash angles that generally exist in the region of the tail at subsonic speeds, relatively large tails are required for stability. At supersonic speeds, tail-rearward configurations generally become stable longitudinally and are, in fact, usually stable with the tail off. Hence, not only is a download required from the tail but also, because of the high stability levels at supersonic speeds, relatively large deflections of the tail are required for trimming and a loss in trim lift-drag ratio similar to that for tailless configurations is experienced.

One approach toward a solution to the trimming problem is through the use of tail-forward or canard arrangements since, for stable configurations, such arrangements require uploads for trimming. Previous investigations of canard arrangements at supersonic speeds (refs. 1 and 2) have indicated that significant gains in trim lift-drag ratio through a reduction in the losses due to trimming might be obtained with these arrangements.

Another approach toward alleviating the trimming problem is through the use of rearward controls located outboard of the wing tips so as to



be in the region of upwash from the wing-tip vortex. For configurations of this type that are unstable with the tail off, the upload required from the tail for trimming is aided by the upwash so that relatively small tails are required. In addition, in an upwash field, the upload at the tail is obtained with a negative deflection and the lift vector from the tail will be inclined forward and thus provide a drag reduction with increasing angle of attack. Some subsonic tests of outboard-tail models are presented in reference 3 together with a discussion of some of the basic concepts and applications of outboard tail designs.

In order to obtain some insight into the relative merits of canard and outboard-tail control systems at supersonic speeds, a preliminary investigation of a generalized canard and outboard-tail model has been conducted in the Langley 4- by 4-foot supersonic pressure tunnel at a Mach number of 2.01 and the results are presented herein.

The canard configuration had a 67° swept wing with an aspect ratio of 2.17 and a trapezoidal canard surface. The outboard-tail model was evolved from the same body-wing configuration used for the canard model by shearing back the outer 30 percent of the wing span to form the boom-mounted outboard-tail panels. The models were tested primarily in pitch with various control deflections although some limited sideslip data were obtained. In addition, some results for various combinations of model component parts were obtained.

SYMBOLS

The results are presented as force and moment coefficients with lift, drag, and pitching moment referred to the stability axis system and rolling moment, yawing moment, and side force referred to the body-axis system. The reference center of moments (center-of-gravity positions) are indicated in figure 1.

C_L	lift coefficient, $Lift/qS$
C_D	drag coefficient, $Drag/qS$
C_m	pitching-moment coefficient, $Pitching\ moment/qS\bar{c}$
C_l	rolling-moment coefficient, $Rolling\ moment/qSb_w$
C_n	yawing-moment coefficient, $Yawing\ moment/qSb_w$
C_y	side-force coefficient, $Side\ force/qS$

q	free-stream dynamic pressure, lb/sq ft
S	total area of wing (including body intercept) for canard model or wing and horizontal tail for outboard-tail model, 1.278 sq ft
c	local chord, in.
\bar{c}	mean geometric chord of wing for canard model or wing plus horizontal tail for outboard-tail model, 11.27 in.
b_w	span of wing for canard model or wing plus horizontal tail for outboard-tail model, 20 in.
M	free-stream Mach number
α	angle of attack, deg
β	angle of sideslip, deg
δ_c	canard control deflection, positive when trailing edge is down, deg
i_t	outboard-tail control deflection, positive when trailing edge is down, deg
L/D	lift-drag ratio
Components:	
B	body
W	wing
V	vertical tail
C	canard surface
b	booms
H	outboard horizontal-tail surface

MODELS AND APPARATUS

Details of the models are shown in figures 1 and 2 and the geometric characteristics are presented in table I. Coordinates for the body are given in table II. The canard model had a trapezoidal canard surface with

hexagonal sections 3 percent thick. A single vertical tail with 3-percent-thick hexagonal sections was mounted on the afterbody of the canard model. The outboard-tail model had horizontal- and vertical-tail panels with 4-percent-thick hexagonal sections. The twin vertical tails had a total exposed area equal to that for the single tail of the canard model and the tail length was the same for both models. The booms for the outboard-tail model had conical noses and cylindrical midsections and were arbitrarily faired into a square cross section in the vicinity of the tails.

The canard control surface could be manually set at angles from 0° to about 15° in approximately 5° increments. The outboard tails could be manually set at angles from 0° to about -10° in approximately 2.5° increments.

The outboard-tail model was formed by removing a portion of the wing tips from the wing used for the canard model and adding the equivalent area and plan form of these tip portions in the form of outboard tail panels. Thus the total area and span of the wing plus tail for the outboard-tail model was the same as that for the wing of the canard model.

Force measurements were made through the use of a six-component internal strain-gage balance.

TESTS, CORRECTIONS, AND ACCURACY

The tests were conducted in the Langley 4- by 4-foot supersonic pressure tunnel at a Mach number of 2.01, a stagnation pressure of 1,440 pounds per square foot, and a stagnation temperature of 110° F. The Reynolds number based on \bar{c} was 2.26×10^6 . The stagnation dewpoint was maintained sufficiently low (-25° F or less) so that no significant condensation effects were encountered in the test section.

Pitch tests of the complete models covered an angle-of-attack range from -4° to about 17° for the canard model and from -4° to about 10° for the outboard-tail model. Sideslip tests were made for an angle-of-sideslip range from -4° to 10° at $\alpha = 0^\circ$ for the canard model and at $\alpha = 0^\circ$ and 10.3° for the outboard-tail model.

The angles of attack and sideslip have been corrected for deflection of the sting and balance under load. The base pressure for the body was measured and the drag for both models was adjusted to a base pressure equal to free-stream static pressure. No base-pressure measurements were made for the booms on the outboard-tail model; however, estimates of the magnitude of the base drag of the booms indicate a relatively small effect on the total drag.

The estimated accuracy of the individual measured quantities is as follows:

C_L	±0.0017
C_D	0.0003
C_m	0.0003
C_z	0.0001
C_n	0.0001
C_y	0.0007
α , deg	0.1
β , deg	0.1
δ_c , deg	0.1
i_t , deg	0.1

DISCUSSION

In order to expedite this investigation, the models used were formed for the most part from existing components. Although neither configuration represents an optimum design, it is believed that the models should be useful for the purpose of comparing the general aerodynamic characteristics of the two widely different configurations and control systems. At the outset it might be well to point out certain factors that might be considered in comparing the two configurations. The outboard-tail model, for example, provides a configuration having more total volume than the canard model since the booms might be considered as sources of available volume for fuel or armament. Also, the vertical- and horizontal-tail surfaces of the outboard-tail model were made 4 percent thick because of model design requirements whereas the vertical-tail and wing-tip portions of the canard model were 3 percent thick.

On the other hand, the canard model provided a greater total lifting surface area since the area of the canard surface is not included with the outboard-tail model. In addition, a portion of the minimum drag increase provided by the canard surface may be attributed to an increase in drag resulting from boundary-layer transition. Estimates based on tests of the body alone, with and without transition fixed by the addition of a band of roughness particles near the nose, indicated that about one-half of the minimum drag increment provided by the canard surface may be due to transition of the boundary layer. This increment of drag was not encountered by the outboard-tail model since it was tested without fixed transition.

Effect of Component Parts

Canard model.- The aerodynamic characteristics in pitch for various combinations of component parts of the canard model are shown in figure 3. The addition of the vertical tail to the body-wing configuration has only a small effect on the longitudinal characteristics consisting primarily of a slight increase in minimum drag and a slight decrease in maximum L/D . The addition of the canard surface provides a large reduction in longitudinal stability and accentuates the tendency toward instability at higher lifts. In addition, the canard surface provides a further increase in drag and decrease in maximum L/D .

Outboard-tail model.- The aerodynamic characteristics in pitch for various combinations of component parts of the outboard-tail model are shown in figure 4. The addition of the booms to the body-wing configuration results in an increase in the lift-curve slope and an increase in longitudinal stability. In addition, the booms cause a substantial increase in minimum drag and reduction in maximum L/D . The addition of the vertical tails primarily results in a further small increase in minimum drag and a reduction in maximum L/D .

The addition of the outboard horizontal tail surfaces provides a large increase in lift-curve slope and in the longitudinal stability. The outboard tails also cause a small increase in minimum drag, but, since the tail is located in an upwash field, the drag due to lift is considerably reduced until the drag for the complete model becomes less and the L/D greater than that for the body-wing configuration at lift coefficients above 0.18.

The experimentally determined variation of effective downwash ϵ with angle of attack for the outboard-tail model is shown in figure 5. The effective downwash was determined from the variation of C_m with α with the horizontal tail off and with the horizontal tail on at various values of i_t . At the intersections of the tail-off curve with the tail-on curves (where the tail provides no pitching moment) it is assumed that the tail is aligned with the local stream angle and the downwash angle is determined from the relation $\epsilon = \alpha + i_t$. The resulting values (fig. 5) indicate the expected negative variation of ϵ with α or an effective upwash flow at the tail.

Effect of Control Deflection

Canard model.- The aerodynamic characteristics in pitch for the canard model with various control deflections are presented in figure 6. Deflection of the canard control surface provides a slight increase in

lift but also causes a considerable increase in drag and consequently a reduction in L/D .

The variation of C_m with C_L is very nonlinear. The static margin near zero lift is about 11 percent, but, at lift coefficients above about 0.35, a condition of essentially neutral stability is indicated. However, the maximum values of L/D occur at lift coefficients below that for which neutral stability occurs.

Outboard-tail model.- The aerodynamic characteristics in pitch for the outboard-tail model with various control deflections are shown in figure 7. Deflection of the outboard-tail control results in a decrease in lift and an increase in minimum drag. However, since the outboard tail is located in a region of upwash from the wing-tip vortex, the drag due to lift decreases substantially with increasing control deflection and, as a result, very little decrease in maximum L/D occurs. Similar to the canard model, the configuration indicates a tendency toward instability at lift coefficients above that for the maximum L/D .

Longitudinal Trim Characteristics

Because of the differences in stability level with the center of gravity at a constant body station, it is apparent that a comparison of the two configurations must involve shifting the center-of-gravity position to provide varying degrees of stability. For this purpose, the maximum trim values of L/D as a function of static stability near zero lift $(\partial C_m / \partial C_L)_0$ are shown in figure 8 for the two configurations. These curves were obtained from figures 6 and 7 by determining the value of $(\partial C_m / \partial C_L)_0$ required to provide trim ($C_m = 0$) at the lift coefficient for maximum L/D for each control deflection. The values of lift coefficient at which the maximum trim L/D occurs are also shown in figure 8.

The stability levels for maximum trim L/D shown in figure 8 do not take into account the changes in stability that occur at higher lifts resulting from the nonlinear moment variation with lift. However, this factor of nonlinear moment variations, which places a limit on the minimum value of $(\partial C_m / \partial C_L)_0$ that can be tolerated before instability at high lifts occurs, will be taken into consideration in the subsequent discussion.

The values of maximum trim L/D decrease as the stability level increases for both configurations (fig. 8), although the variation of maximum trim L/D with stability level is less for the outboard-tail

model than for the canard model. Within the range of this investigation, the values of maximum L/D are relatively high for both configurations, the canard model providing higher values in the lower stability level range and the outboard-tail model providing higher values in the higher stability level range.

For the purpose of comparing the variations of trimmed L/D with lift coefficient for the two configurations, three values of stability level have been chosen. These are for $(\partial C_m / \partial C_L)_0 = 0, -0.11, \text{ and } -0.18$. The variations of trimmed L/D for these three conditions are shown in figure 9. (The pitching-moment curves used in the determination of the variations of trimmed L/D are included in figures 6 and 7.)

For $(\partial C_m / \partial C_L)_0 = 0$ (neutral stability), the configurations are trimmed with zero control deflection through most of the lift range and hence, the comparison of L/D variations is essentially the same as a comparison of the variations of untrimmed L/D for δ_c or $i_t = 0$. These results (fig. 9) indicate higher values of L/D throughout the lift range for the canard model than for the outboard-tail model. However, as indicated by the tick marks on the curves, pitch-up instability is indicated near the lift coefficient for maximum L/D for the canard model and at a lift coefficient somewhat higher than that for maximum L/D for the outboard-tail model.

For $(\partial C_m / \partial C_L)_0 = -0.11$, the values of maximum trim L/D are the same for the two models but occur at a lower lift coefficient for the canard model than for the outboard-tail model. The pitch-up limit for the canard model is increased to a value somewhat greater than that for the outboard-tail model.

For $(\partial C_m / \partial C_L)_0 = -0.18$, the maximum L/D is slightly higher and occurs at a higher lift for the outboard-tail model than for the canard model. No pitch-up was encountered for either configuration within the trim limits of the investigation although the indications are that pitch-up might occur for the outboard-tail model at slightly higher lifts (fig. 7(b)).

It is apparent that a comparison of the relative merits of the two configurations must take into consideration a number of factors such as the allowable stability level, the required lift coefficient for trim, and the pitch-up limitations. However, an inspection of figures 8 and 9 indicates some distinct characteristics for each configuration. For example, throughout the range of the investigation, the values of trim L/D were higher in the low-lift range and the maximum L/D occurs at a lower lift coefficient for the canard configuration than for the outboard-tail configuration. At higher lift coefficients, the values of trim L/D

(for conditions of positive stability) become higher for the outboard-tail configuration. These effects reflect the drag characteristics of the two configurations wherein the outboard-tail configuration has a higher minimum drag but a lower drag due to lift than the canard configuration.

The fact that the maximum value of L/D occurs at a higher lift coefficient for the outboard-tail configuration than for the canard configuration would mean that, for a given stability level, in order to operate at maximum L/D , the outboard-tail configuration would require either a higher wing loading or a higher altitude.

An additional factor to consider is that for a constant center-of-gravity position the outboard-tail model has a considerably higher stability level than the canard model (figs. 7(a) and 6(a)). Hence, for the same longitudinal stability the center-of-gravity position must be farther rearward for the outboard-tail model and should be considered in the requirements for maintaining directional stability. The farther rearward center-of-gravity position required for the outboard-tail model may result in some benefits from the standpoint of take-off and landing since wing trailing-edge flaps would be located near the center of gravity and they could thus provide increased lift with little increase in pitching moment. The stability level indicated by the outboard-tail configuration could be altered by relocating the tail or by varying the tail area but the effects of these variables on the aerodynamic characteristics have not been determined.

Lateral Stability

Directional stability.- The sideslip characteristics at $\alpha = 0^\circ$ (fig. 10) indicate that for the test center-of-gravity position (body station 21.97) the canard model and the outboard-tail model have approximately the same level of directional stability. This result would be expected since the two models have the same tail volume. However, in order to obtain equal longitudinal stability levels, it is necessary to shift the center-of-gravity positions of the two configurations. The effect of this shift on the directional stability at $\alpha = 0^\circ$ is included in figure 10(b) wherein the variation of C_n with β is presented for various constant values of longitudinal stability. As would be expected, the level of directional stability for equal longitudinal stability is less for the outboard-tail model because of the farther rearward center-of-gravity position required. At $\alpha = 10.3^\circ$ (fig. 11), the level of directional stability for the outboard-tail model is reduced slightly although positive directional stability is maintained even for the lowest value of longitudinal stability (fig. 11(b)). Although no directional stability tests were made for the canard model above $\alpha = 0^\circ$, it would

be expected that the directional stability for the canard configuration would also decrease with increasing angle of attack.

Effective dihedral.- The canard model at $\alpha = 0^\circ$ (fig. 10(a)) indicates a positive dihedral effect $(-C_{l\beta})$ that results from the side force on the vertical tail. The outboard-tail model, however, indicates a slightly negative dihedral effect at $\alpha = 0^\circ$ (fig. 10). In this case the positive dihedral effect to be expected from the side force on the vertical tails is apparently offset by an interference effect induced by the flow field of the vertical tail on the outboard horizontal-tail panels. Further evidence of this effect is indicated at $\alpha = 10.3^\circ$ (fig. 11(a)) wherein the addition of the vertical tails provides only a small increment of effective dihedral in spite of a large increment in side force. The interference flow field from the vertical tails to the outboard horizontal tails is such that a positive pressure is transmitted to the upper surface of the upwind horizontal-tail panel whereas a negative pressure is transmitted to the upper surface of the downwind horizontal-tail panel. Because of the moment arm involved, these pressures provide a rolling moment about equal to that provided by the vertical tail, but in the opposite direction. Further investigations of these interference fields are necessary to determine the effects of varying the deflection angle of the horizontal and vertical tails.

CONCLUDING REMARKS

An investigation has been made in the Langley 4- by 4-foot supersonic pressure tunnel at a Mach number of 2.01 to determine the stability and control characteristics of a canard configuration and an outboard-tail configuration. The results of the investigation indicated relatively high values of maximum trimmed lift-drag ratio L/D for both configurations. The values of maximum trim L/D decreased as the stability level increased for both configurations, although the variation was less for the outboard-tail model than for the canard model. The values of trim L/D were higher in the low-lift range and the maximum L/D occurred at a lower lift coefficient for the canard configuration than for the outboard-tail configuration. At higher lift coefficients the values of trim L/D became higher for the outboard-tail configuration. These effects reflect the drag characteristics of the two configurations wherein the outboard-tail configuration had a higher minimum drag but a lower drag due to lift than the canard configuration.

Langley Aeronautical Laboratory,
National Advisory Committee for Aeronautics,
Langley Field, Va., January 14, 1958.

REFERENCES

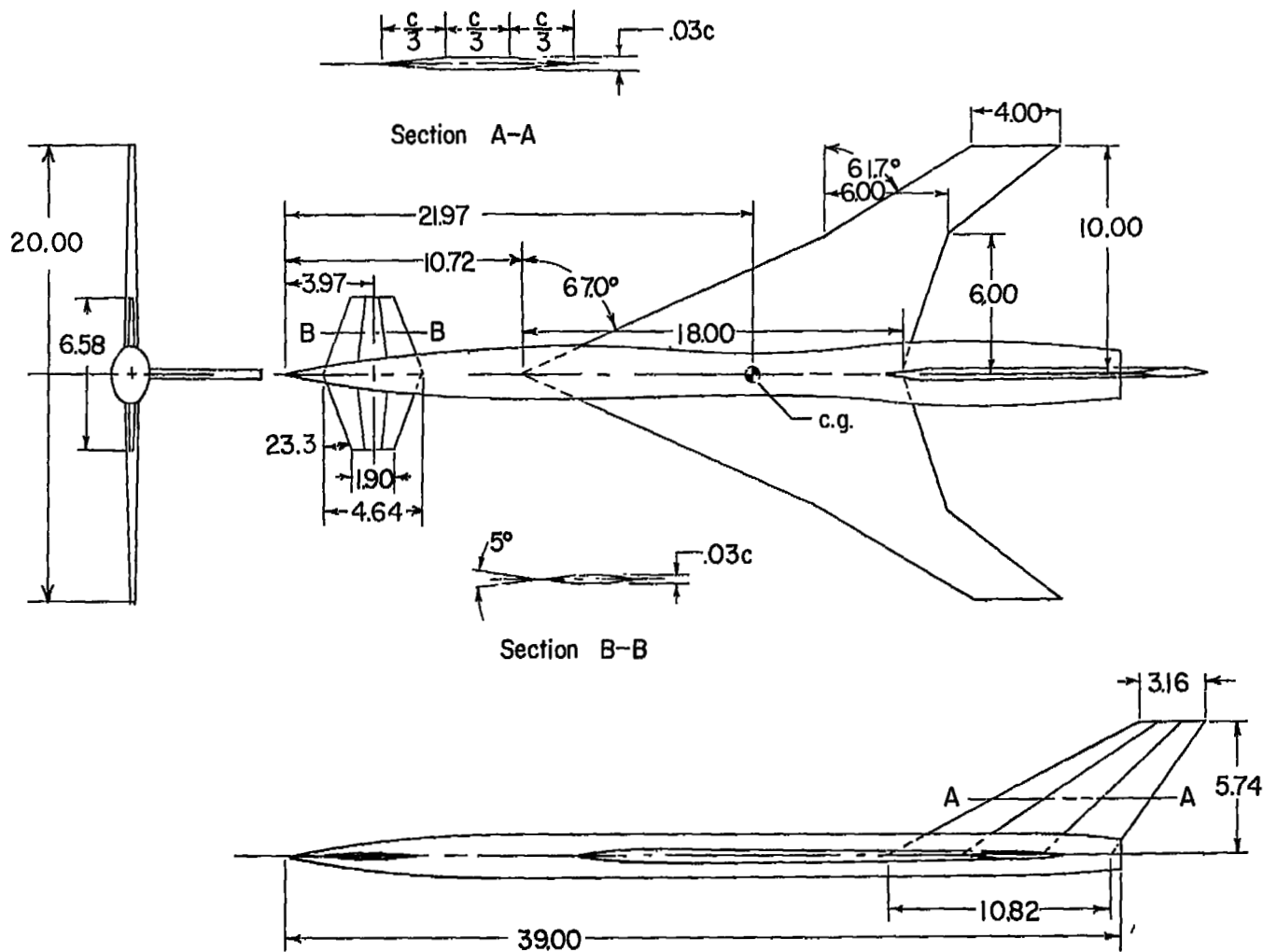
1. Spearman, M. Leroy: Some Factors Affecting the Static Longitudinal and Directional Stability Characteristics of Supersonic Aircraft Configurations. NACA RM L57E24a, 1957.
2. Driver, Cornelius: Longitudinal and Lateral Stability and Control Characteristics of Two Canard Airplane Configurations at Mach Numbers of 1.41 and 2.01. NACA RM L56L19, 1957.
3. Sleeman, William C., Jr.: Preliminary Study of Airplane Configurations Having Tail Surfaces Outboard of the Wing Tips. NACA RM L58B06, 1958.

TABLE I.- GEOMETRIC CHARACTERISTICS OF MODELS

Wing (canard model):		
Total area, including body intercept, sq ft		1.278
Span, in.		20.00
Mean geometric chord, in.		11.27
Taper ratio, inboard panel		0.333
Taper ratio, outboard panel		0.667
Leading-edge sweep, inboard, deg		67.0
Leading-edge sweep, outboard, deg		61.7
Airfoil section	65A distribution	
Thickness ratio, root, percent		4.00
Thickness ratio, tip, percent		3.20
Aspect ratio		2.17
Root chord, in.		18.00
Tip chord, inboard panel, in.		6.00
Tip chord, outboard panel, in.		4.00
Wing (outboard-tail model):		
Area, inboard of boom, including body intercept, sq ft		1.00
Span, in.		12.00
Aspect ratio		1.00
Canard:		
Area, exposed, sq in.		14.96
Span, total, in.		6.58
Tip chord, in.		1.90
Root chord at body center line, in.		4.64
Taper ratio		0.41
Leading-edge sweep, deg		23.3
Midchord sweep, deg		0
Airfoil section	Hexagonal	
Thickness ratio, percent		3.00
Horizontal tail:		
Area, exposed, both panels, sq in.		29.50
Span, exposed, each panel, in.		3.00
Tip chord, in.		4.00
Root chord, exposed, in.		5.50
Taper ratio		0.73
Aspect ratio, each panel		0.61
Leading-edge sweep, deg		61.7
Airfoil section	Hexagonal	
Thickness ratio, percent		4.00
Vertical tail:		
	Body mounted	Wing mounted
		(Each)
Area to center line	40.15	18.52
Span to center line, in.	5.74	3.85
Tip chord, in.	3.16	2.24
Root chord at center line, in.	10.82	7.37
Taper ratio	0.29	0.30
Aspect ratio	0.82	0.80
Leading-edge sweep angle, deg	65.0	64.7
Airfoil section	Hexagonal	Hexagonal
Thickness ratio, percent	3.00	4.00
Booms:		
Length, in.		19.00
Maximum height, in.		1.00
Maximum width, in.		1.00
Base area, sq in.		1.00
Wing station of boom center line, in.		6.50
Body:		
Length, in.		39.00
Maximum cross-sectional area, sq in.		6.072
Diameter of equivalent circle, in.		2.78
Length-diameter ratio		14.03
Base area, sq in.		2.99

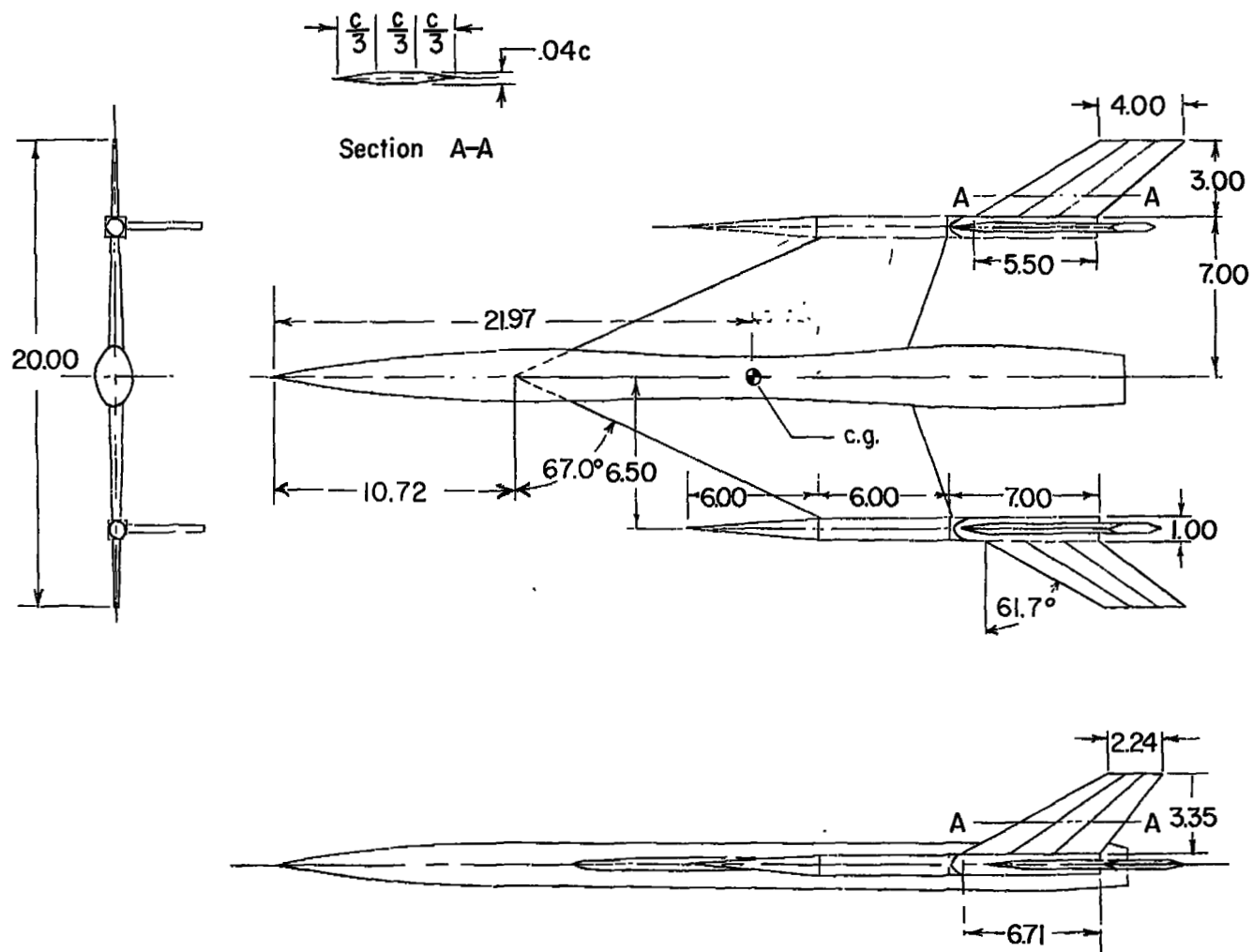
TABLE II.- BODY COORDINATES

Body station, in.	Radius, in.		Body Station, in.	Radius, in.	
	Major axis	Minor axis		Major axis	Minor axis
0	0	0	21	1.325	1.195
1	.297	.198	22	1.257	1.195
2	.492	.328	23	1.198	1.195
3	.655	.437	24	1.211	1.195
4	.799	.533	25	1.260	1.195
5	.928	.619	26	1.332	1.195
6	1.045	.696	27	1.446	1.195
7	1.151	.767	28	1.514	1.195
8	1.248	.832	29	1.542	1.195
9	1.337	.891	30	1.554	1.195
10	1.418	.945	31	1.534	1.195
11	1.492	.995	32	1.489	1.195
12	1.559	1.040	33	1.433	1.195
13	1.620	1.080	34	1.369	1.182
14	1.666	1.116	35	1.303	1.155
15	1.666	1.149	36	1.231	1.117
16	1.645	1.175	37	1.155	1.072
17	1.609	1.190	38	1.067	1.025
18	1.551	1.195	39	.975	.975
19	1.482	1.195			
20	1.399	1.195			



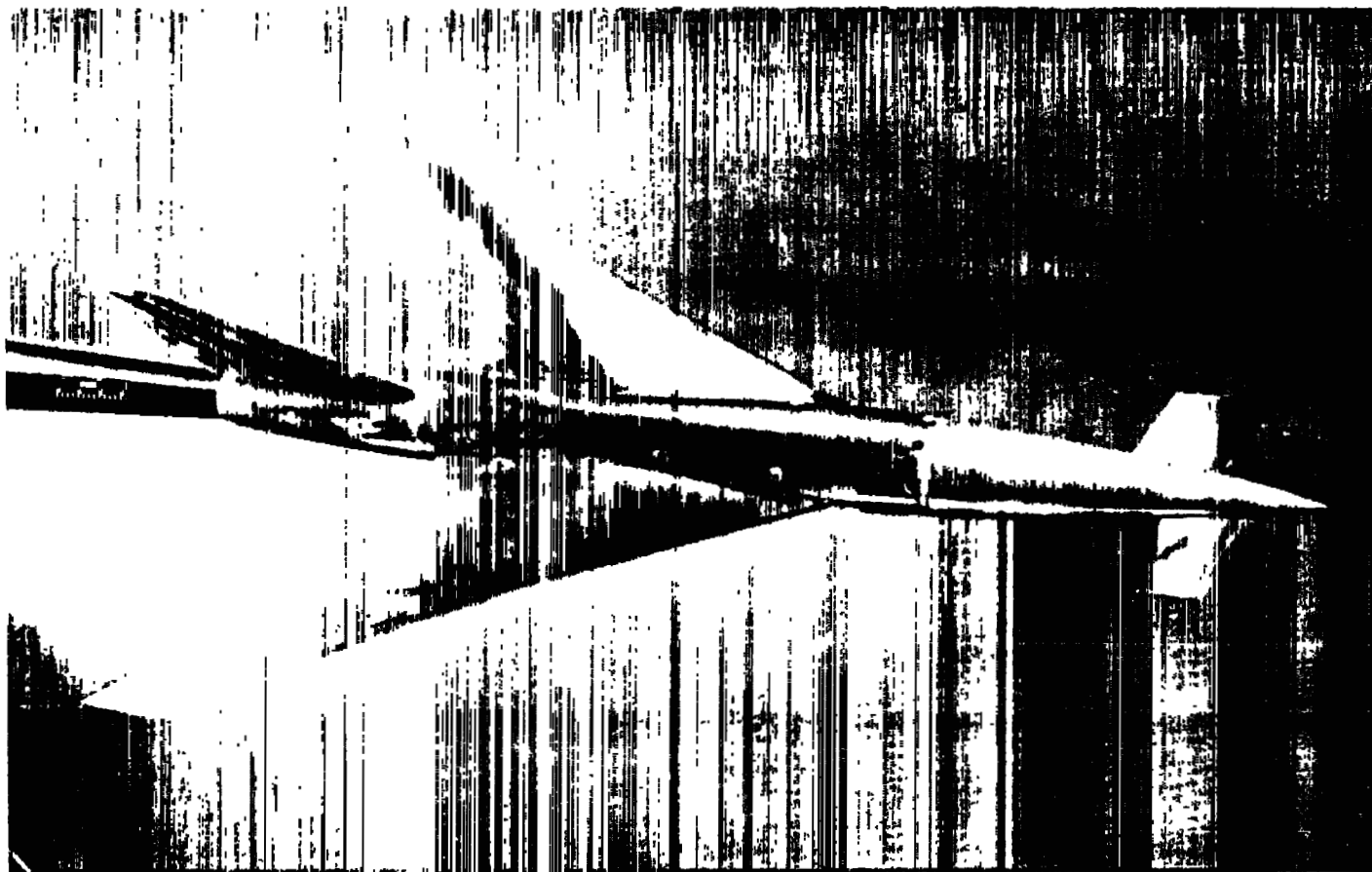
(a) Canard model.

Figure 1.- Details of models.



(b) Outboard-tail model.

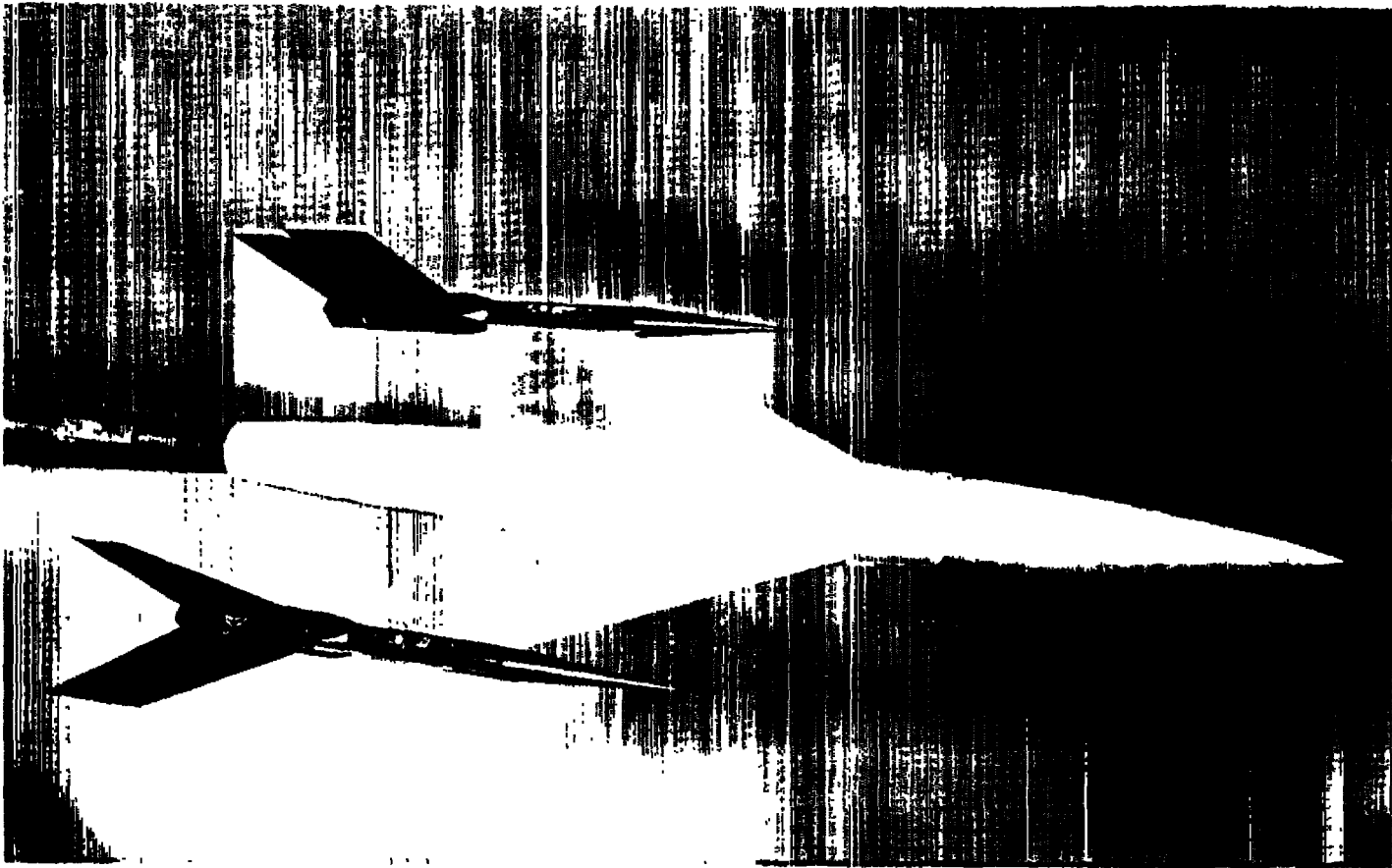
Figure 1.- Concluded.



(a) Canard model.

L-57-3254

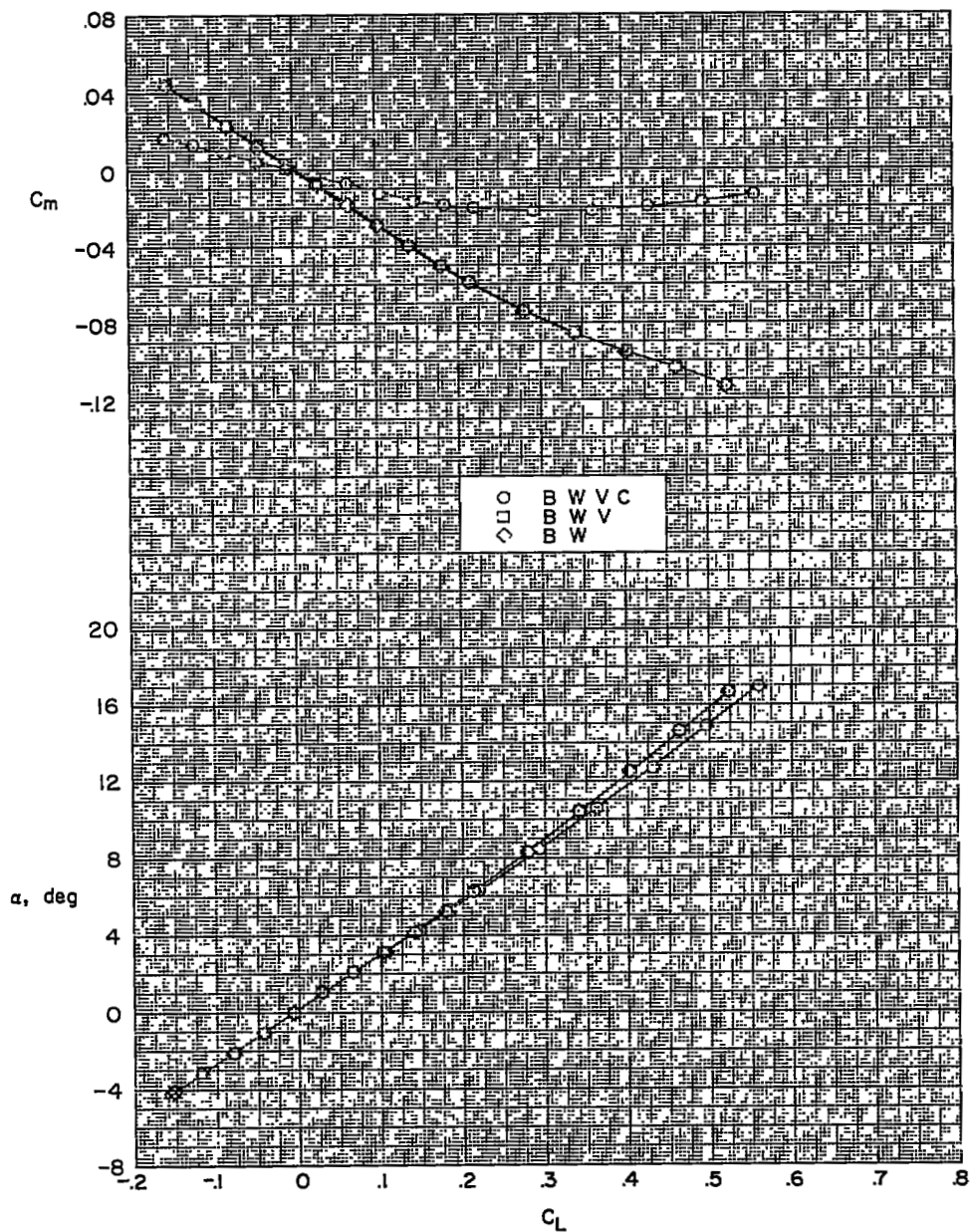
Figure 2.- Photographs of models.



(b) Outboard-tail model.

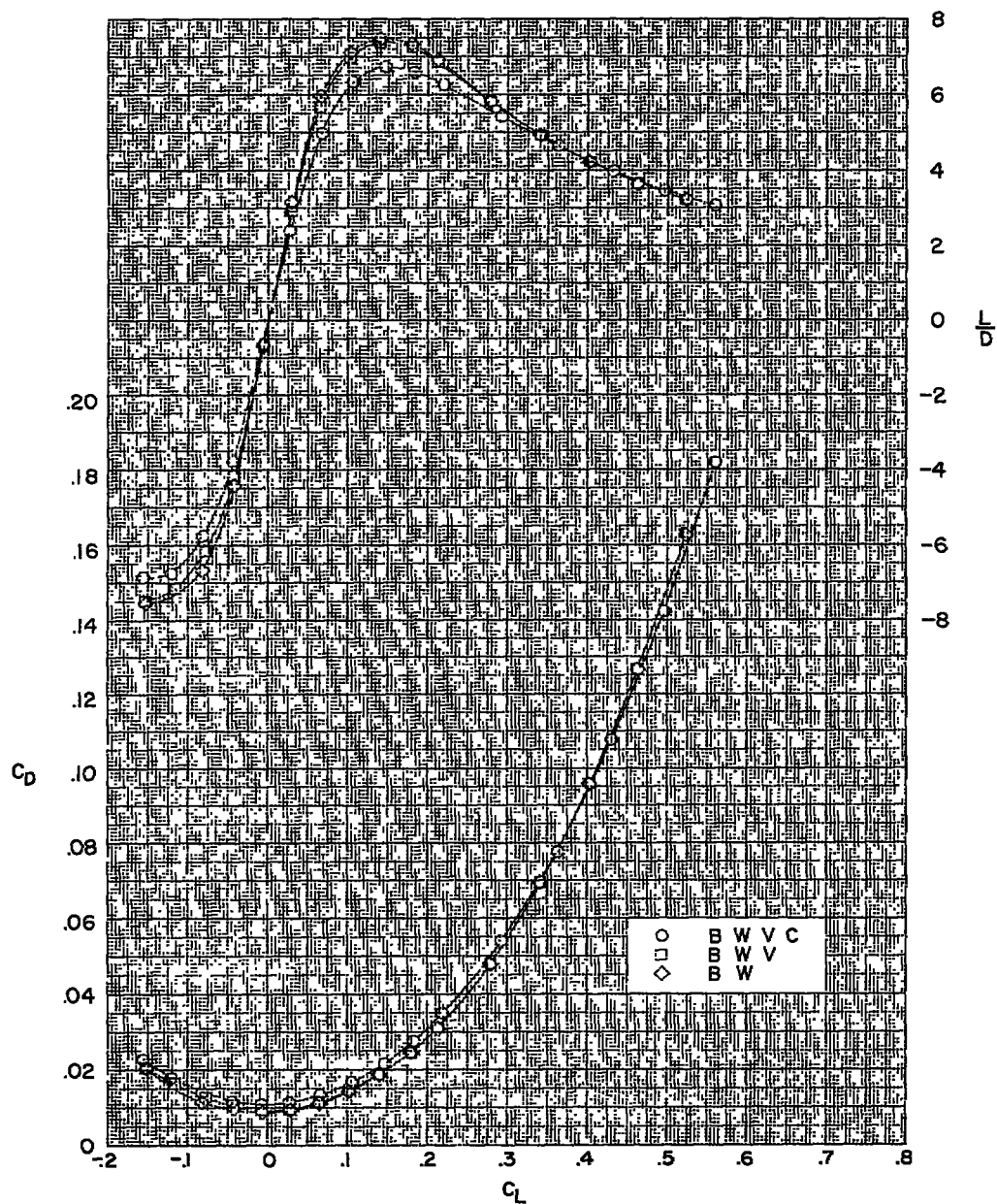
L-57-3253

Figure 2.- Concluded.



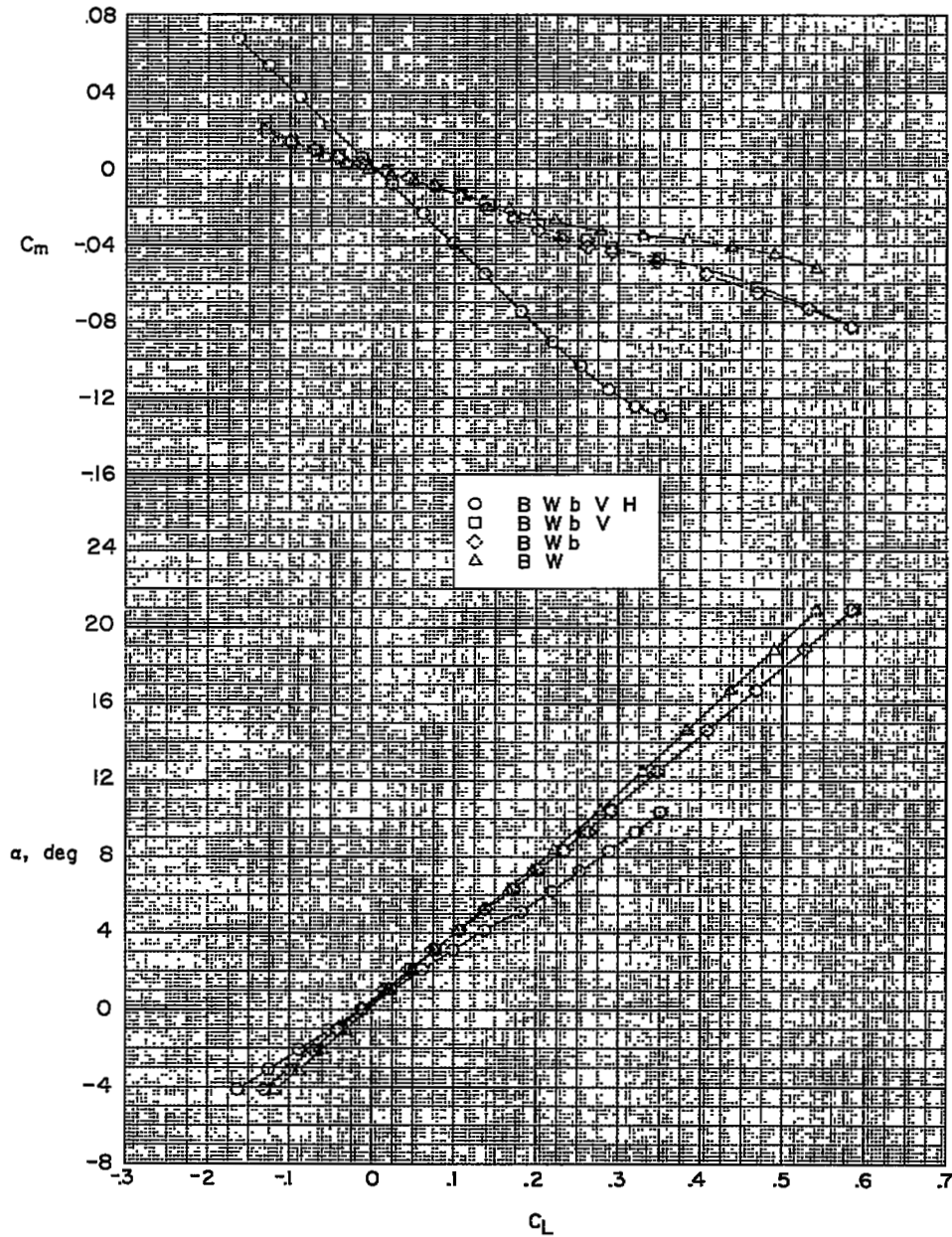
(a) Variation of C_m and α with C_L .

Figure 3.- Aerodynamic characteristics in pitch for various component parts of canard model. $\delta_c = 0^\circ$.



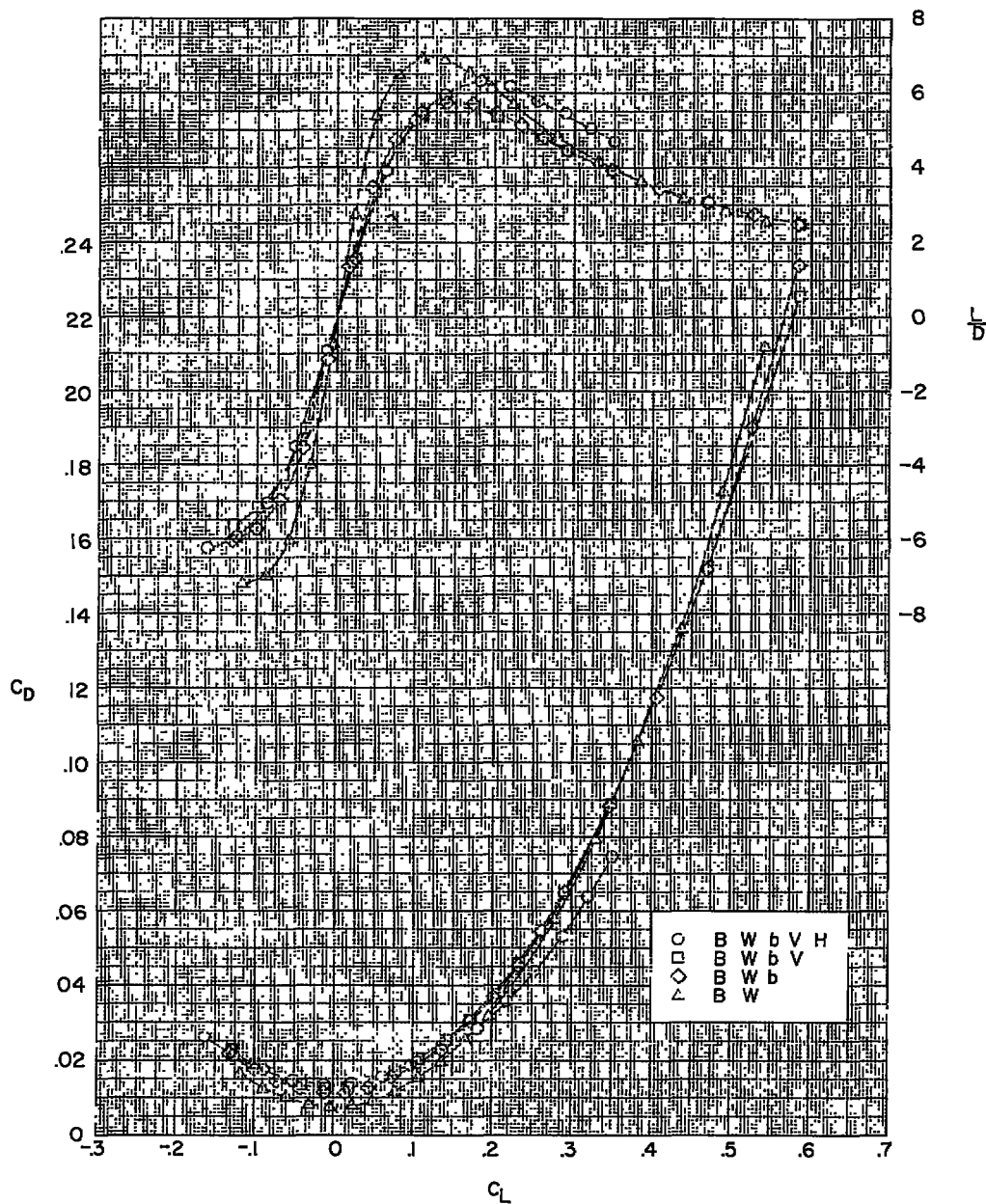
(b) Variation of L/D and C_D with C_L .

Figure 3.- Concluded.



(a) Variation of C_m and α with C_L .

Figure 4.- Aerodynamic characteristics in pitch for various component parts of outboard-tail model. Forward center-of-gravity position; $i_t = 0^\circ$.



(b) Variation of L/D and C_D with C_L .

Figure 4.- Concluded.

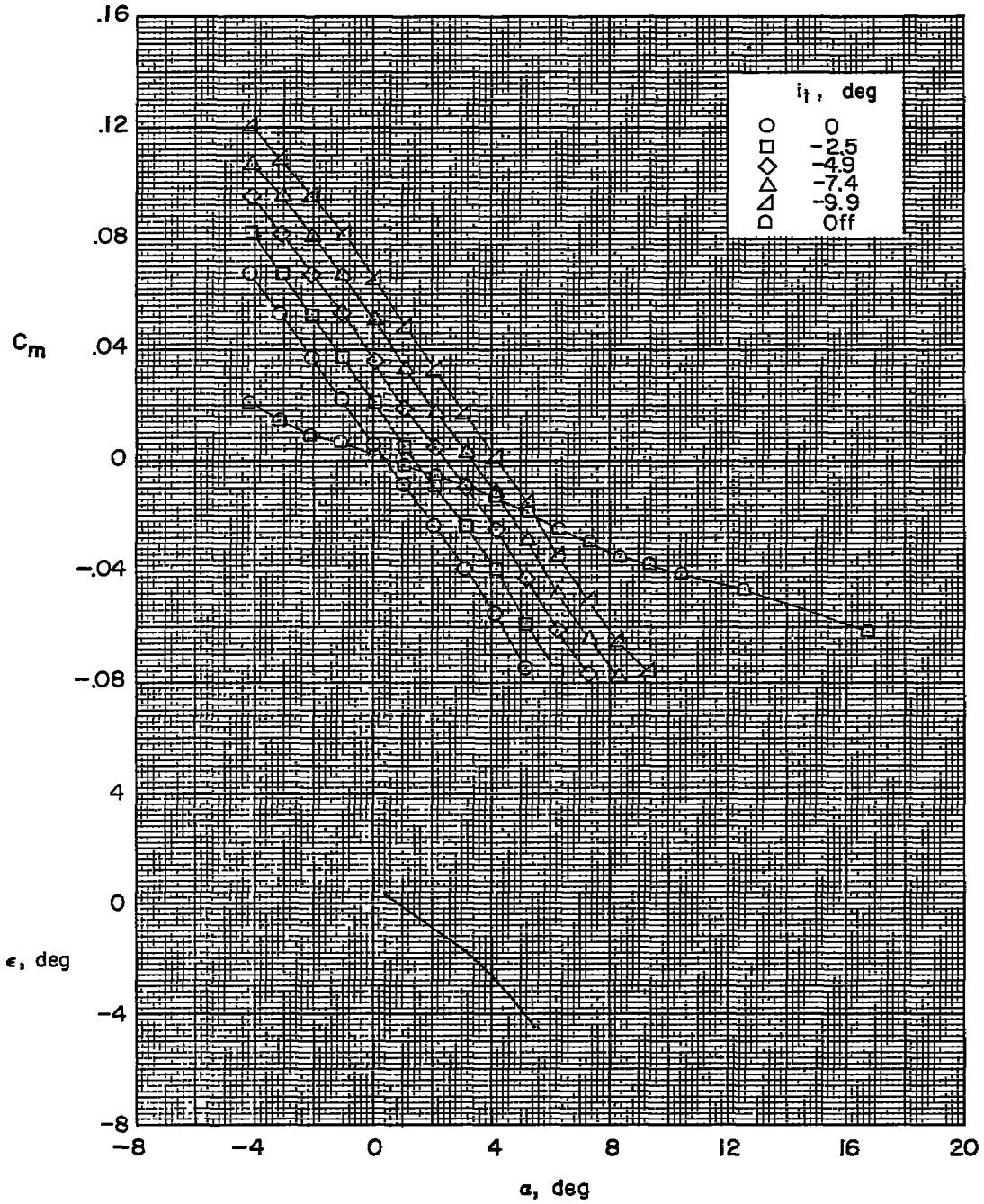
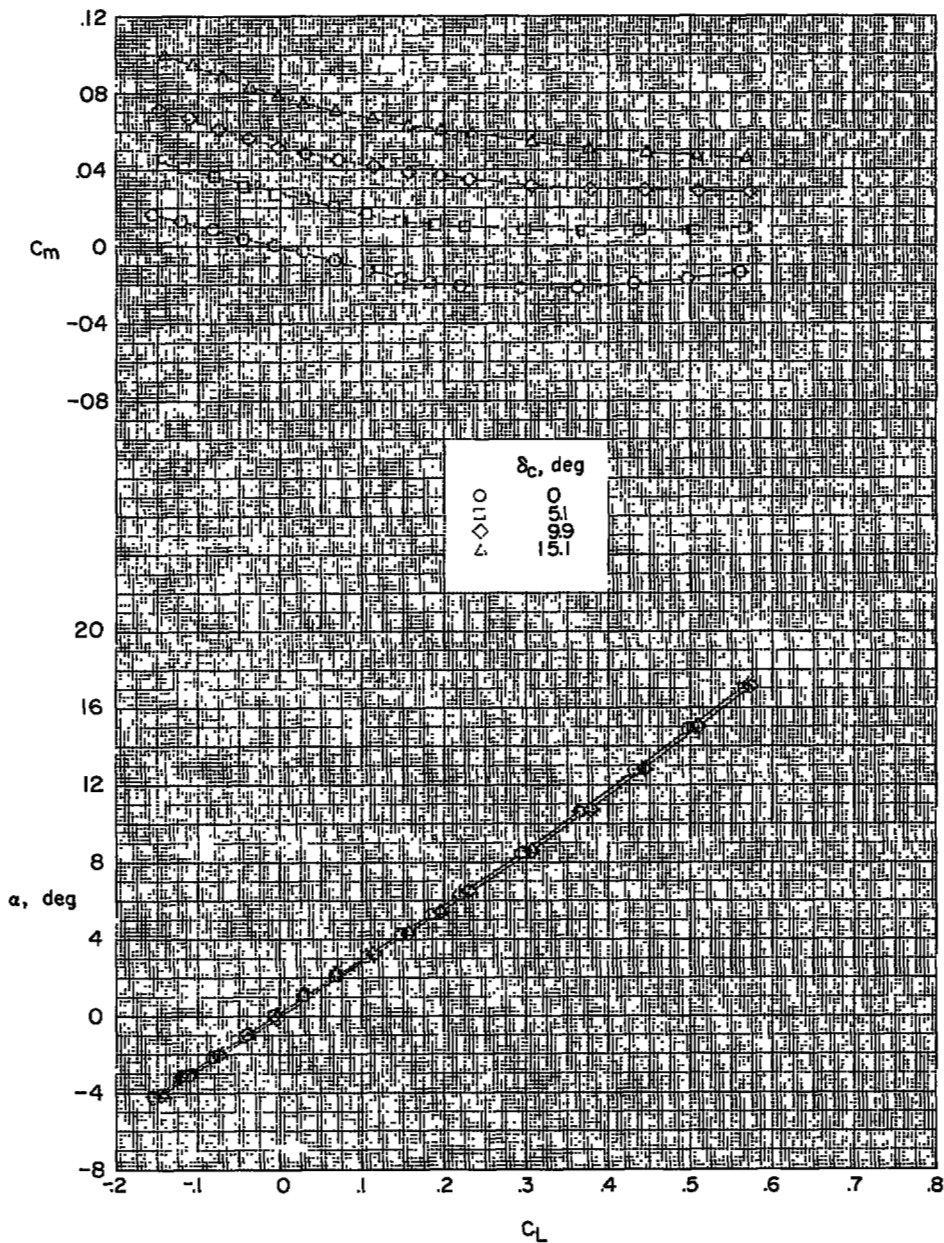
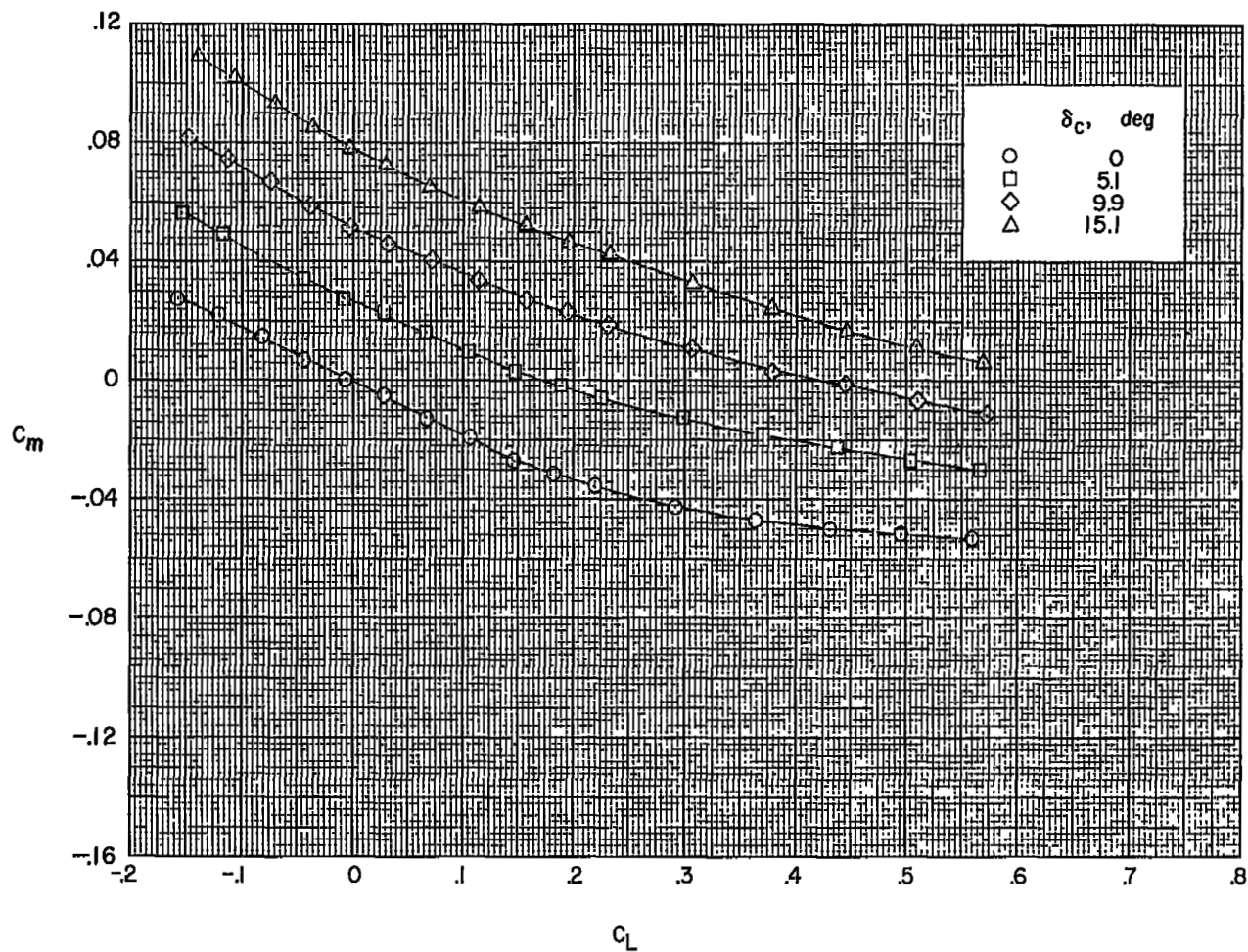


Figure 5.- Effective downwash characteristics for outboard-tail configuration.



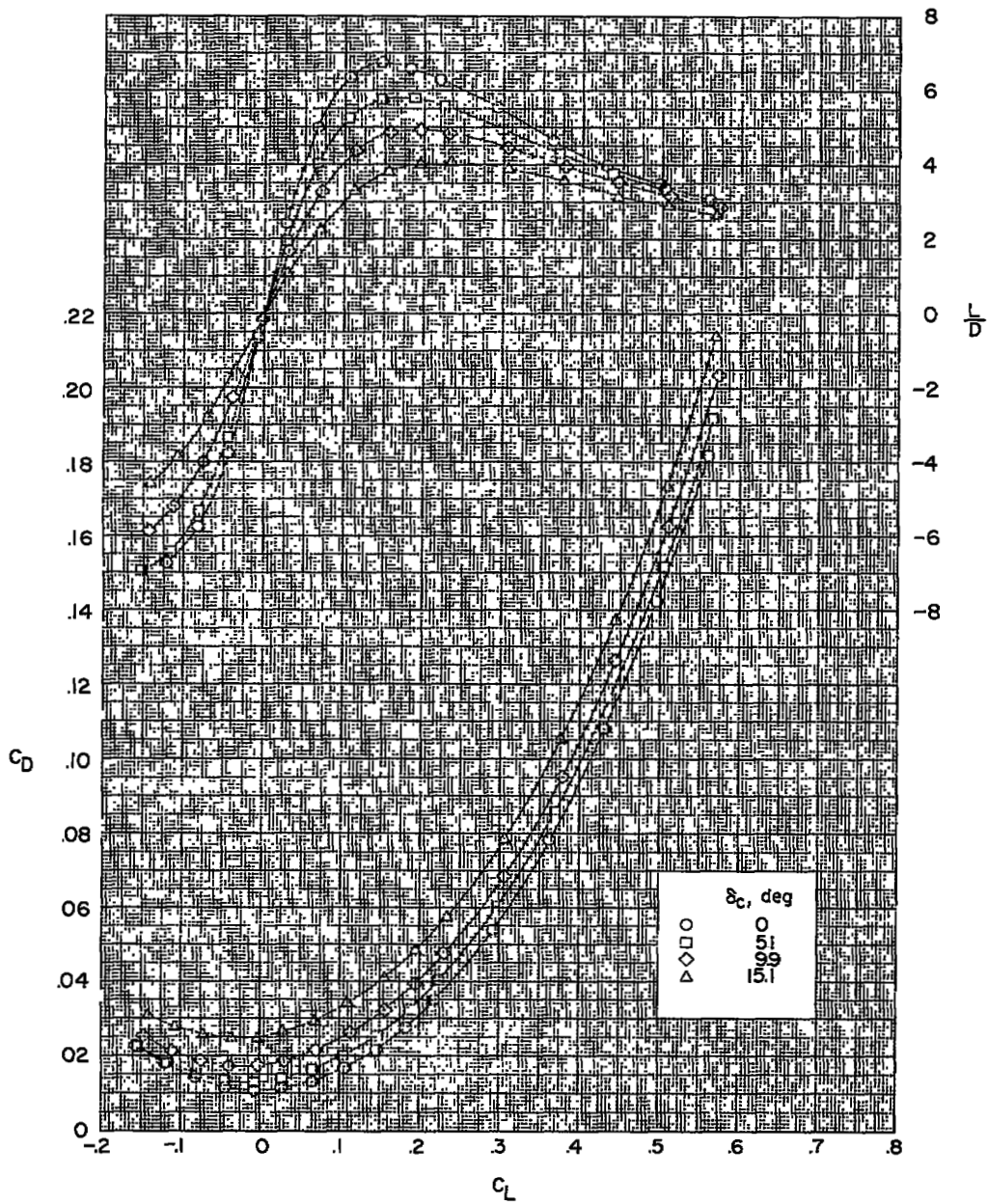
(a) Variation of C_m and α with C_L . $\partial C_m / \partial C_L = -0.11$.

Figure 6.- Aerodynamic characteristics in pitch for canard model with various control deflections.



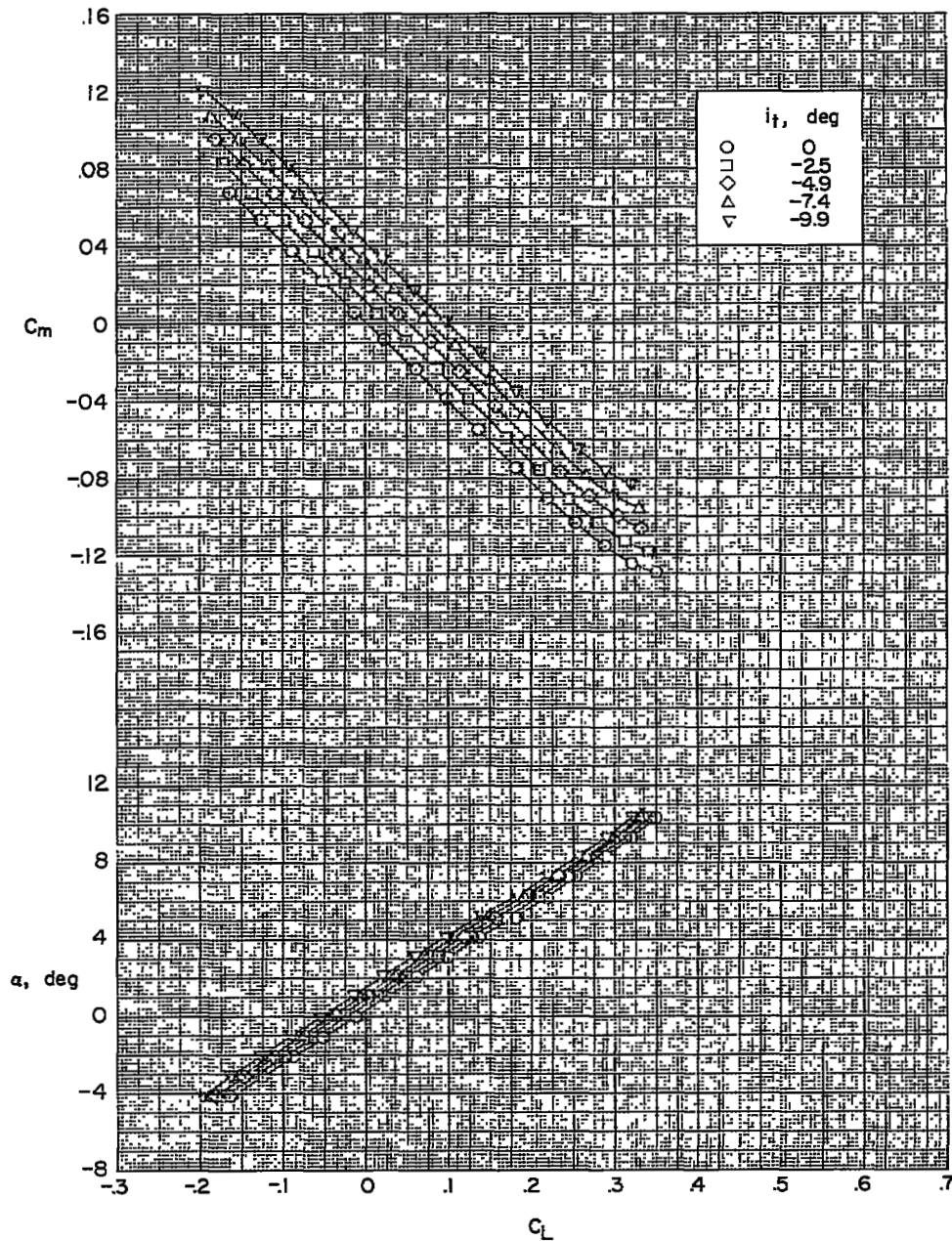
(b) Variation of C_m with C_L . $(\partial C_m / \partial C_L)_0 = -0.18$.

Figure 6.- Continued.



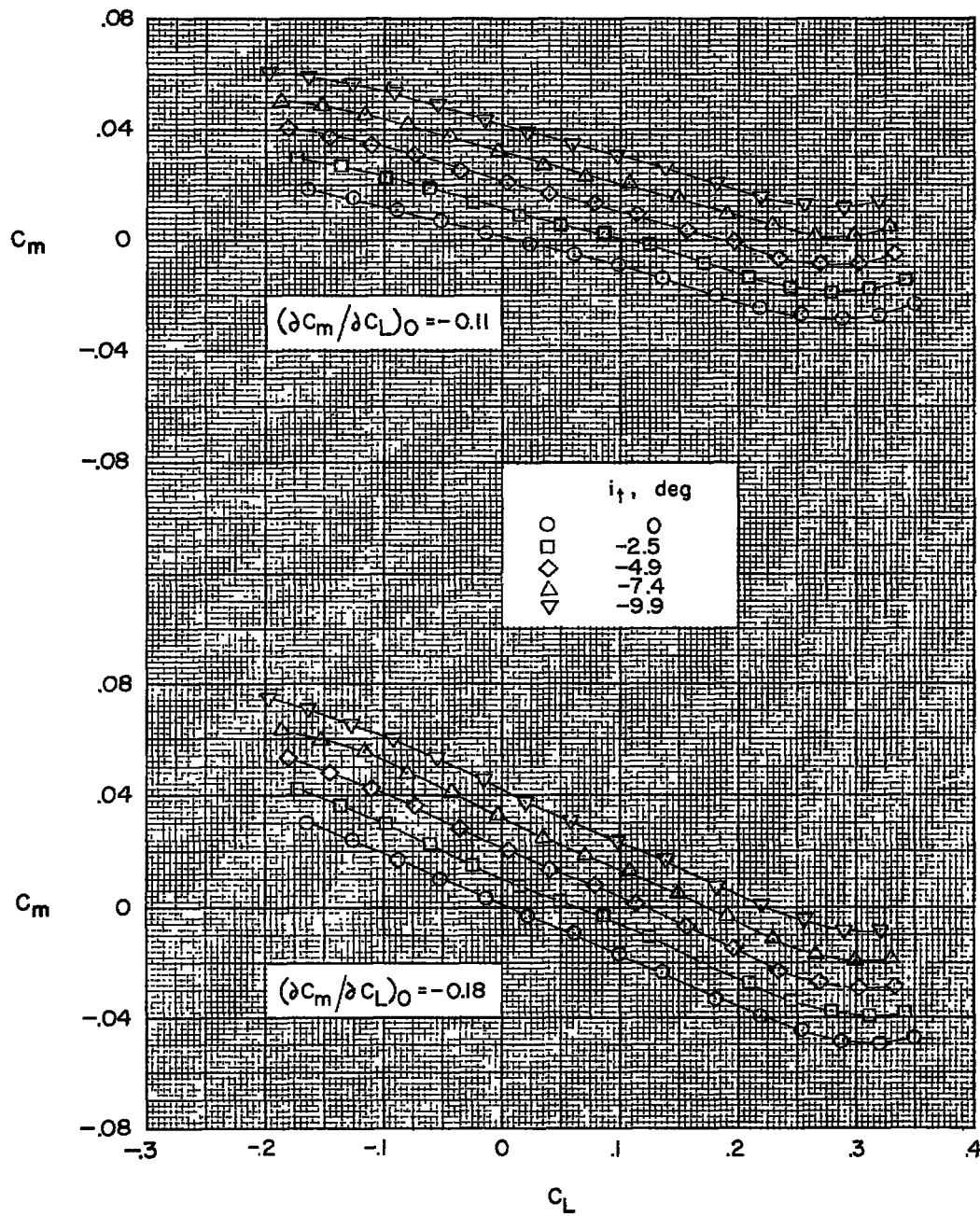
(c) Variation of L/D and C_D with C_L .

Figure 6.- Concluded.



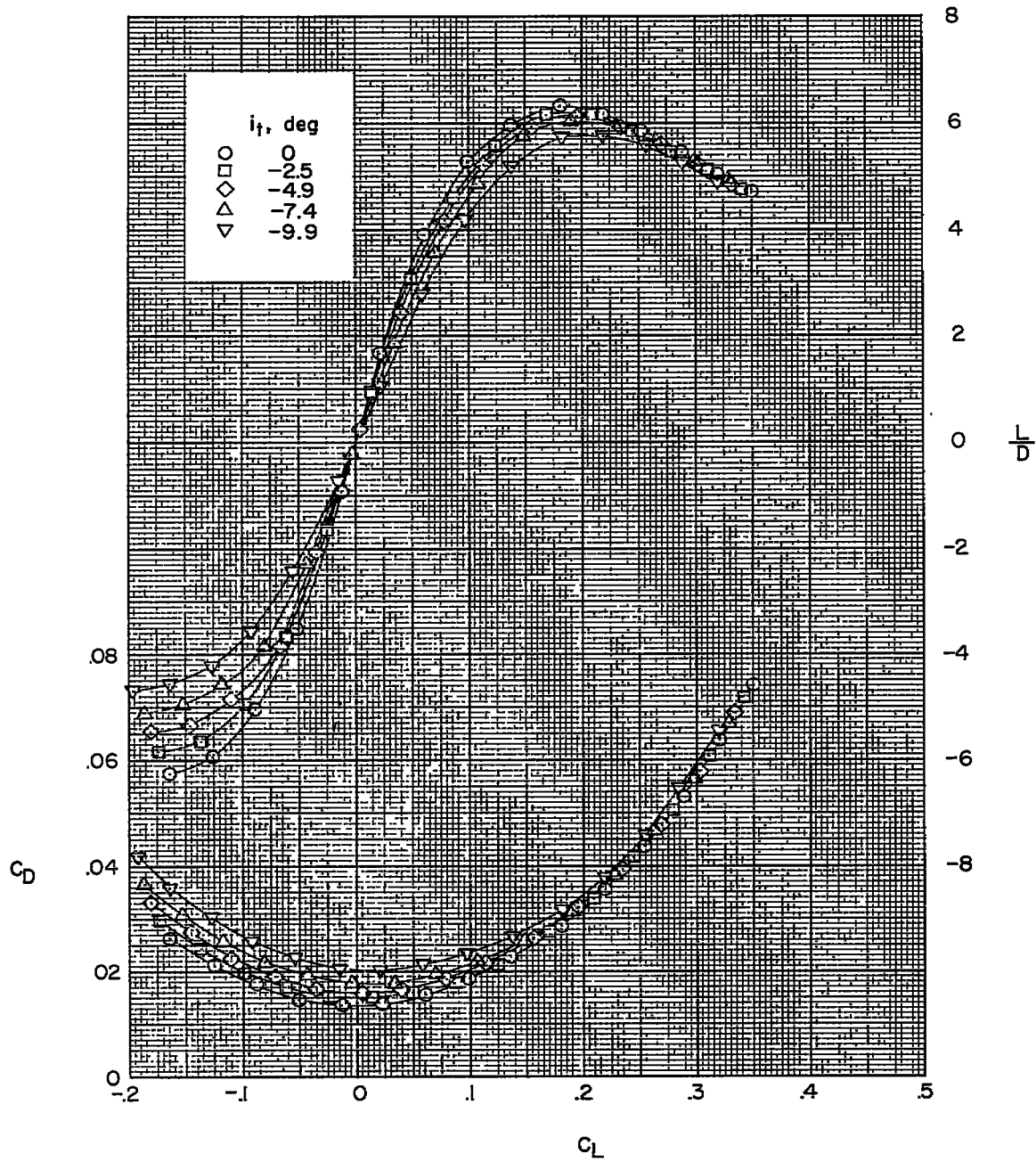
(a) Variation of C_m and α with C_L . $\partial C_m / \partial C_L = -0.41$.

Figure 7.- Aerodynamic characteristics in pitch for outboard-tail model with various control deflections.



(b) $(\partial C_m / \partial C_L)_0 = -0.11$ and -0.18 .

Figure 7.- Continued.



(c) Variation of L/D and C_D with C_L .

Figure 7.- Concluded.

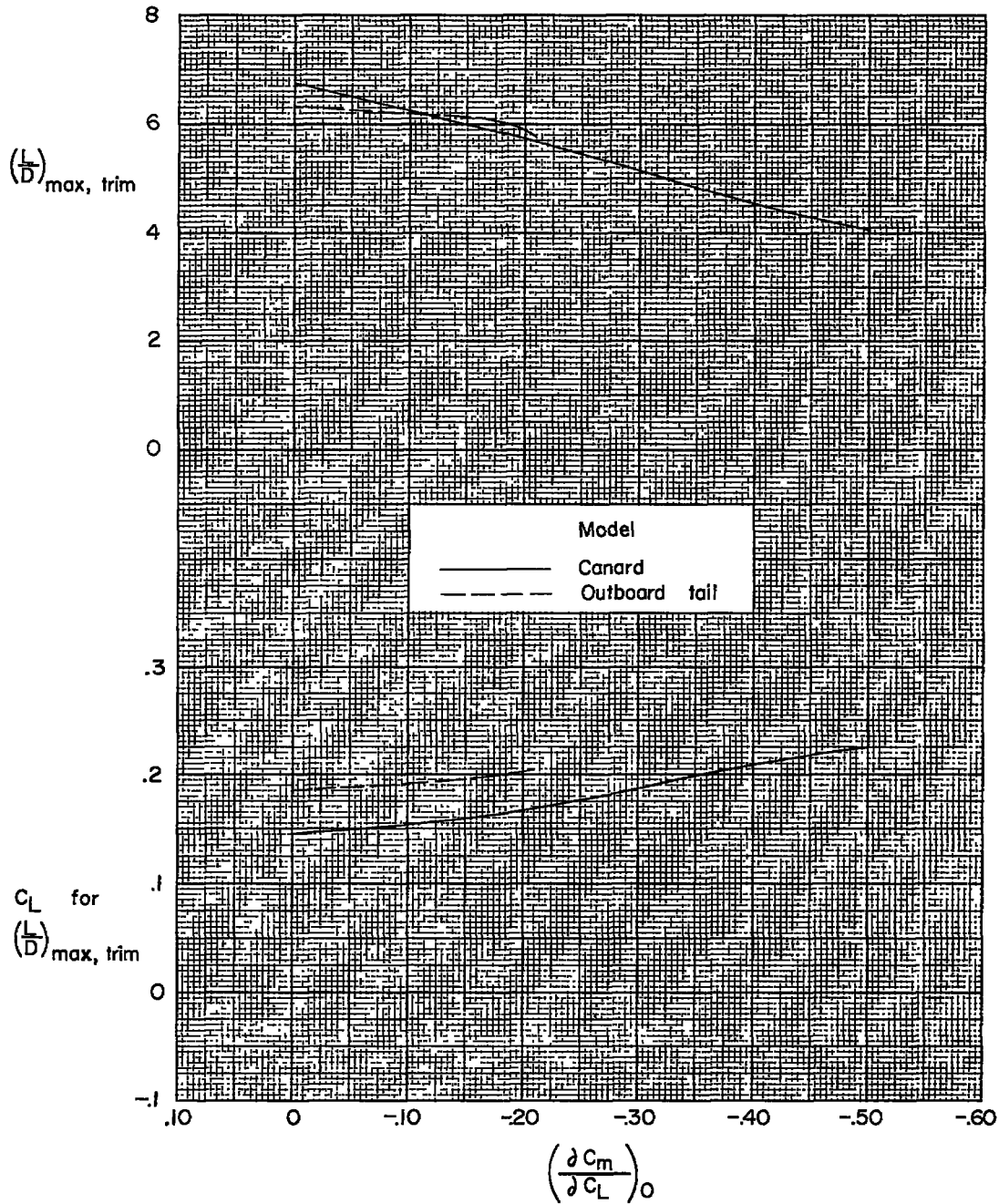


Figure 8.- Trimmed maximum L/D characteristics as a function of longitudinal stability.

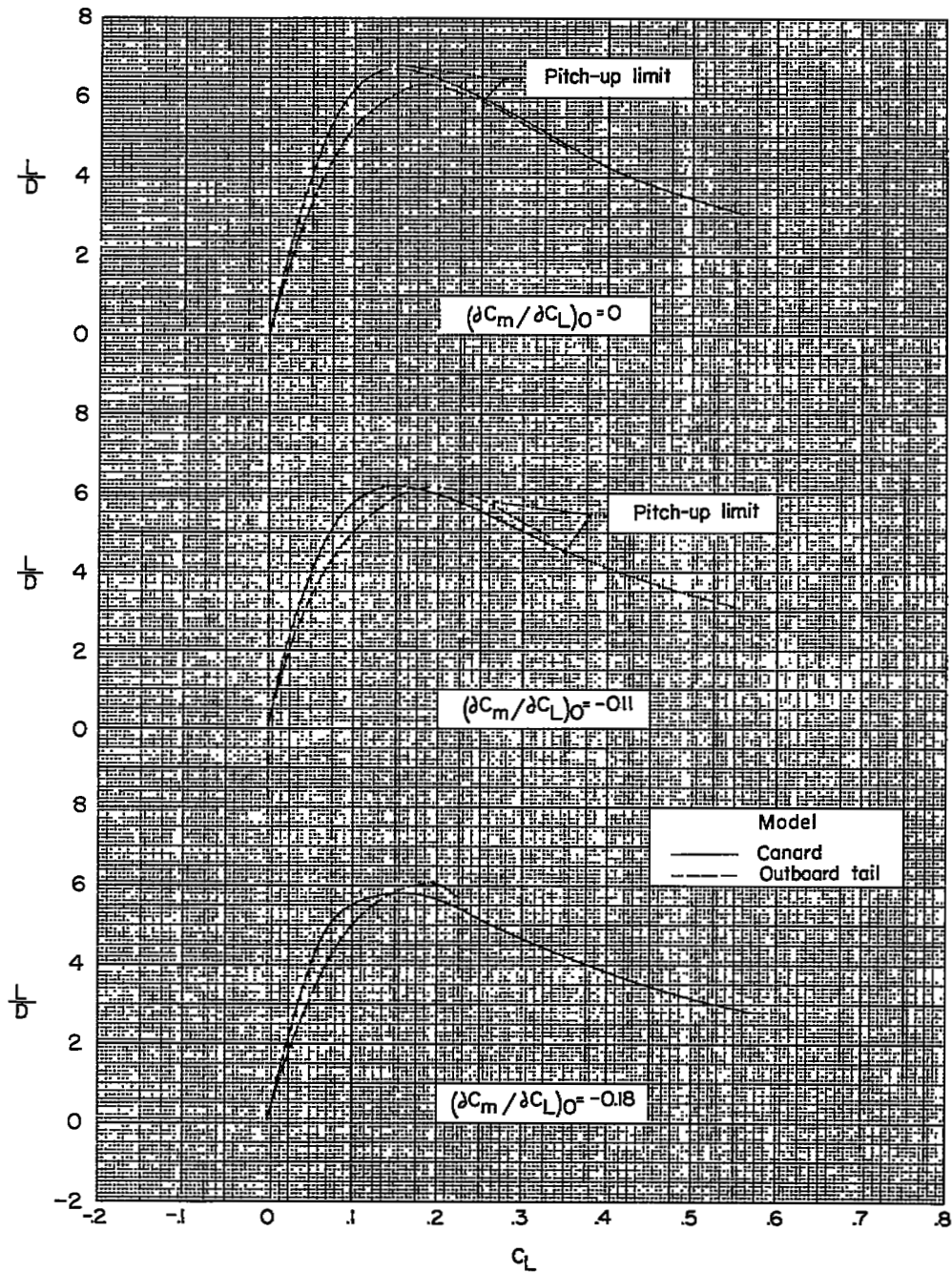
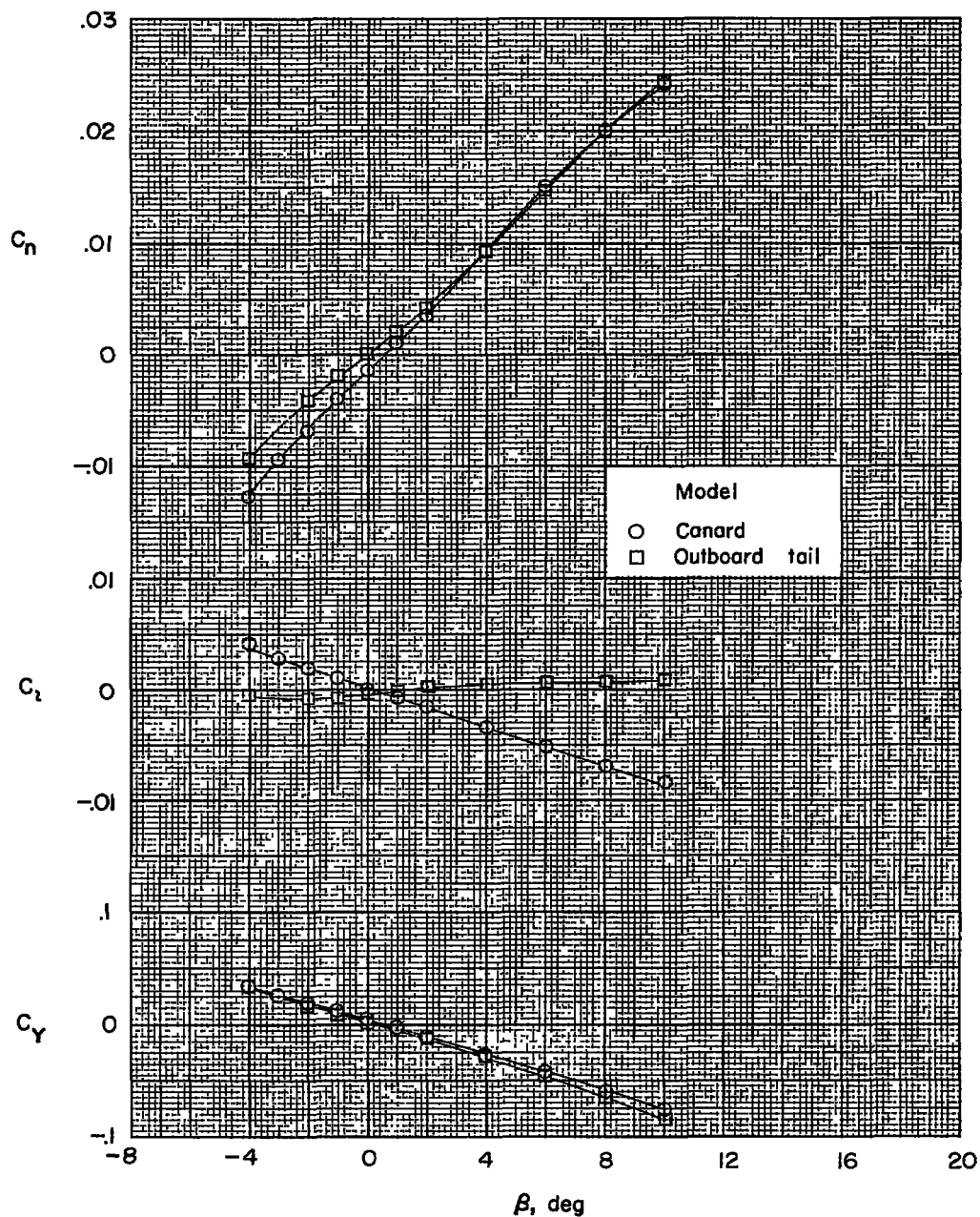
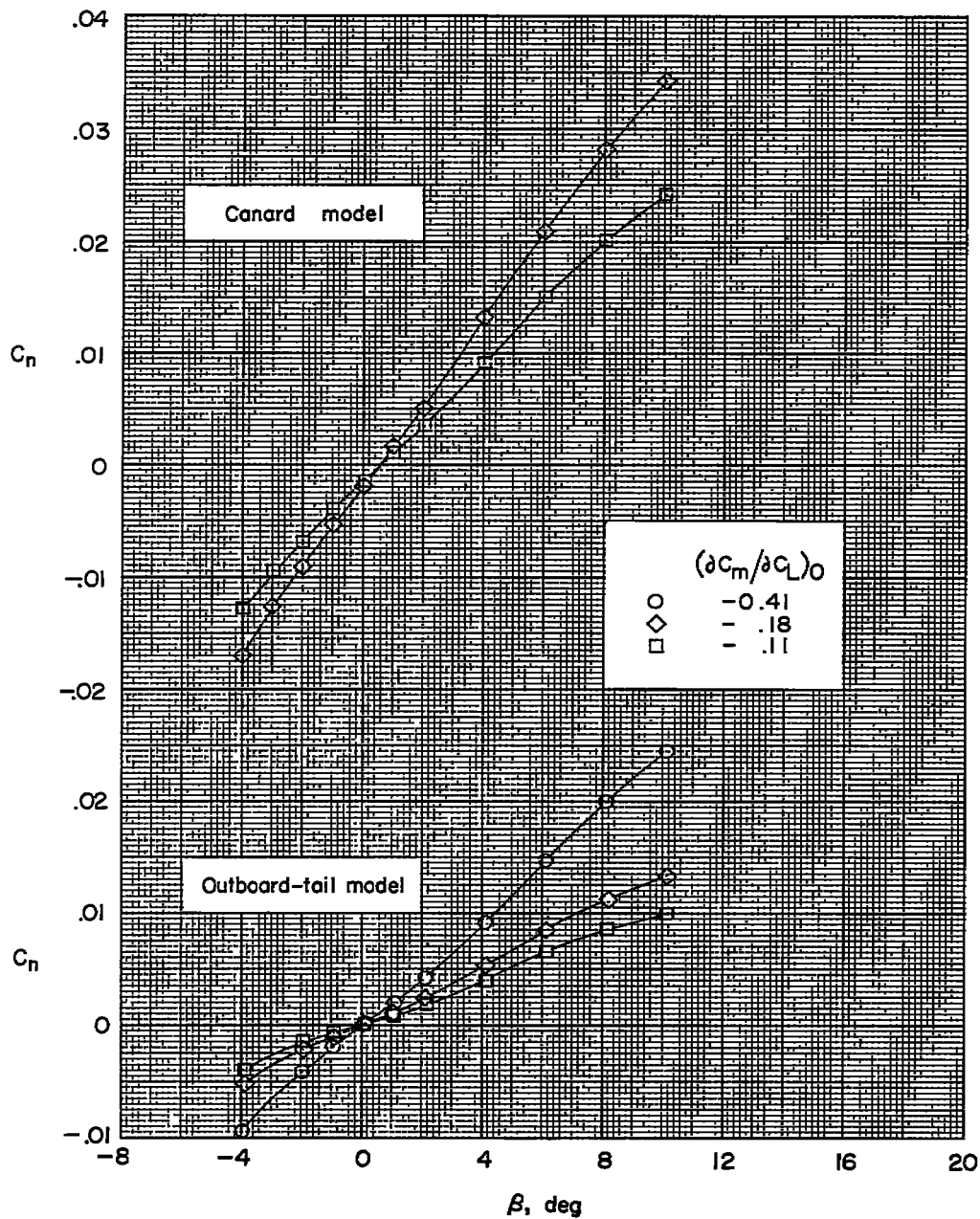


Figure 9.- Variation of trimmed L/D with lift coefficient for various longitudinal stability levels.



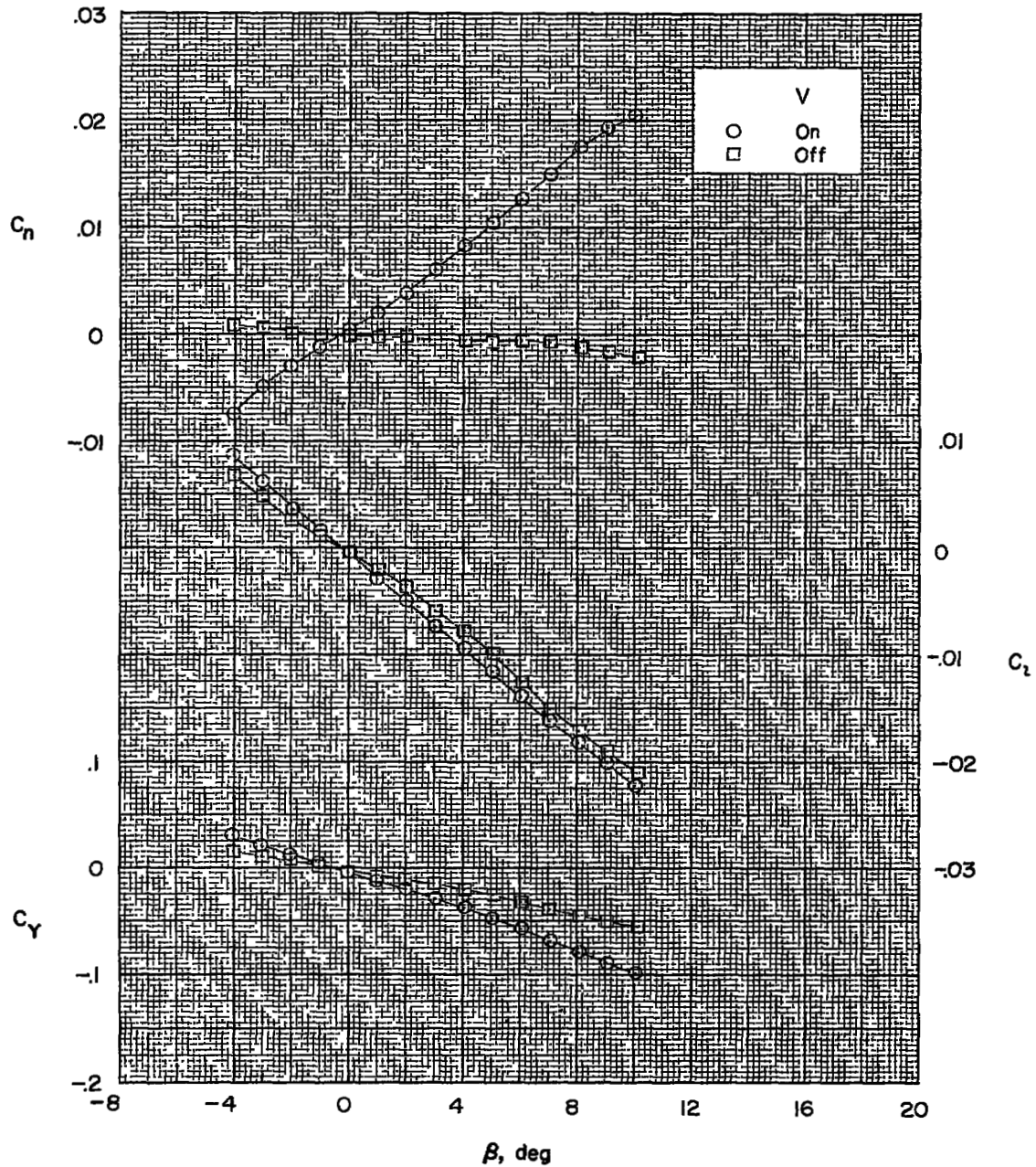
(a) Constant center-of-gravity position at body station 21.97.

Figure 10.- Aerodynamic characteristics in sideslip for canard and outboard-tail models. $\alpha = 0^\circ$.



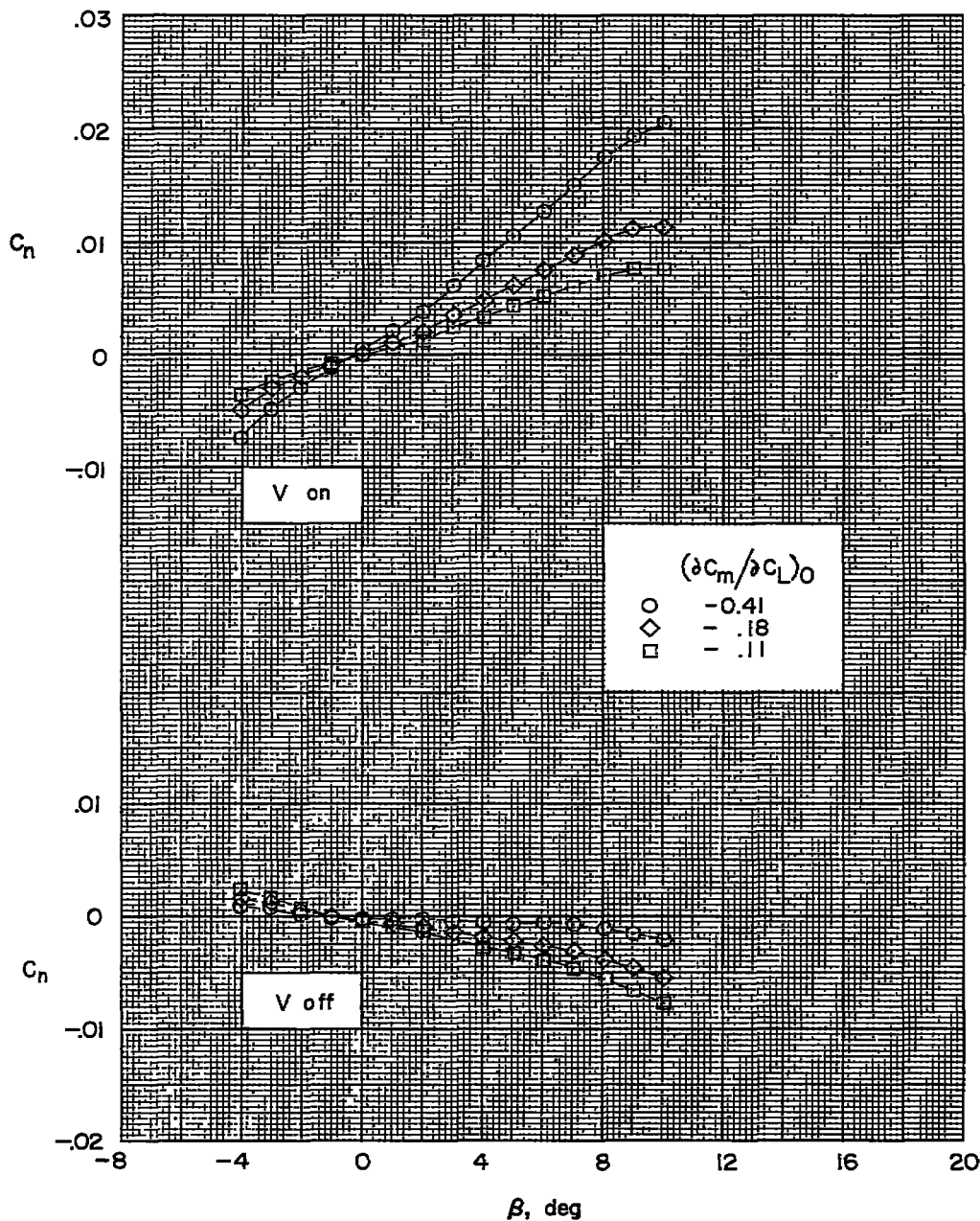
(b) Constant longitudinal stability.

Figure 10.- Concluded.



(a) Center of gravity at body station 21.97.

Figure 11.- Aerodynamic characteristics in sideslip for outboard-tail model. $\alpha = 10.3^\circ$.



(b) Varying center-of-gravity position for different values of longitudinal stability.

Figure 11.- Concluded.